repiSalud
Repositorio Institucional en Salud

This is the peer reviewed version of the following article:

Ramirez, R. J., Takemoto, Y., Martins, R. P., Filgueiras-Rama, D., Ennis, S. R., Mironov, S., . . . Pandit, S. V. (2019). Mechanisms by Which Ranolazine Terminates Paroxysmal but Not Persistent Atrial Fibrillation. *Circulation. Arrhythmia and Electrophysiology, 12*(10), e005557. doi:10.1161/CIRCEP.117.005557

which has been published in final form at: https://doi.org/10.1161/CIRCEP.117.005557

**Mechanisms by which Ranolazine Terminates Paroxysmal but not Persistent Atrial Fibrillation**

Rafael J. Ramirez, PhD,[1]* Yoshio Takemoto, MD, PhD,[1]* Raphaël P. Martins, MD, PhD,[1]* David Filgueiras-Rama, MD,[1,5,6] Steven R. Ennis, PhD,[1] Sergey Mironov, PhD,[1] Sandesh Bhushal, MS,[2] Makarand Deo, PhD,[2] Sridharan Rajamani, PhD,[3,4] Omer Berenfeld, PhD,[1] Luiz Belardinelli, MD,[3] José Jalife, MD,[1,5,6] Sandeep V. Pandit, PhD.[1]

[1] Center for Arrhythmia Research, Department of Internal Medicine-Cardiology, University of Michigan, Ann Arbor, MI, USA
[2] Norfolk State University, Norfolk, VA, USA
[3] Gilead Sciences, Foster City, CA, USA
[4] Currently at: Amgen Inc., San Francisco, CA, USA
[5] Fundación Centro Nacional de Investigaciones Cardiovasculares, Carlos III (CNIC), Madrid, Spain
[6] Centros de Investigación Biomédica en Red (CIBER) for Cardiovascular Diseases, Spain
* Equal Contribution

**Correspondence:**
Rafael J. Ramirez OR Sandeep V. Pandit
Center for Arrhythmia Research
University of Michigan
2800 Plymouth Road
Ann Arbor, MI 48109, USA
Tel: +1-734-998-7500
Fax: +1-734-998-7711
Email: rjramirezjr@gmail.com OR sanpandimich@gmail.com

**Short Title:** Effects of Ranolazine in Atrial Fibrillation
**Word Count:** 5177 (manuscript body only)
**Journal Subject Terms:** Arrhythmias, Atrial Fibrillation, Computational Biology, Electrophysiology, Animal Models of Human Disease, Physiology

**Abstract**

**Background.** Ranolazine inhibits $Na^+$ current ($I_{Na}$), but whether it can convert atrial fibrillation (AF) to sinus rhythm (SR) remains unclear. We investigated antiarrhythmic mechanisms of ranolazine in sheep models of paroxysmal (PxAF) and persistent AF (PsAF). **Methods.** PxAF was maintained during acute stretch (*N*=8), and PsAF was induced by long-term atrial tachypacing (*N*=9). Isolated, Langendorff-perfused sheep hearts were optically mapped. **Results.** In PxAF ranolazine (10 μM) reduced dominant frequency (DF) from 8.3±0.4 to 6.2±0.5 Hz ($p$<0.01) before converting to SR, decreased singularity point (SP) density from 0.070±0.007 to 0.039±0.005 $cm^{-2}s^{-1}$ ($p$<0.001) in left atrial epicardium ($LA_{epi}$), and prolonged AF cycle length (AFCL); rotor duration, tip trajectory and variance of AFCL were unaltered. In PsAF, ranolazine reduced DF (8.3±0.5 to 6.5±0.4 Hz, $p$<0.01), prolonged AFCL, increased the variance of AFCL, had no effect on SP density (0.048±0.011 to 0.042±0.016 $cm^{-2}s^{-1}$, $p$=n.s.) and failed to convert AF to SR. Doubling the ranolazine concentration (20 μM) or supplementing with dofetilide (1 μM) failed to convert PsAF to SR. In computer simulations of rotors, reducing $I_{Na}$ decreased DF, increased tip meandering and produced vortex shedding upon wave interaction with unexcitable regions. **Conclusions.** PxAF and PsAF respond differently to ranolazine. Cardioversion in the former can be attributed partly to decreased DF and SP density, and prolongation of AFCL. In the latter, increased dispersion of AFCL and likely vortex shedding contributes to rotor formation, compensating for any rotor loss, and may underlie the inefficacy of ranolazine to terminate PsAF.

**Keywords:** AF, Paroxysmal, Persistent, Rotors, Wavebreaks, Ranolazine

## Introduction

Atrial fibrillation (AF) is the most common arrhythmia seen in the clinic. It affects ~2 million people in the US and increases the risk of stroke and heart failure.[1] Despite substantial advances in catheter ablation, antiarrhythmic drugs constitute the mainstay for treatment of patients with AF.[2] However, drugs are not always effective and can cause ventricular arrhythmias.[3] The lack of efficacy of drugs in AF is poorly understood and could be related to complex drug/ion channel interactions and electrical (ionic)[4] as well as structural remodeling (fibrosis, dilation, hypertrophy) of the atria.[5] In animal models where AF is induced via tachypacing, electrical remodeling occurs within weeks whereas structural remodeling occurs over months.[4-8] AF in humans has similar characteristics: electrical remodeling occurs in days, and once stabilized, shortening of atrial action potential duration (APD) is independent of AF duration (3 weeks–3 years).[9] Conversely, changes in atrial extracellular matrix correlate with AF duration: structural remodeling is more severe in permanent than in persistent AF, and less pronounced in hearts without AF.[10] Efficacy of antiarrhythmic drugs for either cardioversion or maintenance of sinus rhythm (SR) is decreased with long-duration AF in both animal models[11] and humans.[12] However, the underlying mechanisms remain unclear, and this has motivated the search for new, more potent antiarrhythmic drugs for use in patients with AF.

Among the new antiarrhythmic strategies under consideration for AF are drugs that selectively target ion channels in the atria, or with biophysical properties that are distinct from their ventricular counterparts.[13] This strategy is attractive because it is less likely to provoke life threatening ventricular arrhythmias.[12,13] An emerging focus has been atrial $Na^+$ current ($I_{Na}$), which has been reported to display a higher density, and more negative steady-state inactivation characteristics compared to ventricular $I_{Na}$ in animal models.[14] The anti-anginal drug ranolazine has been shown to preferentially inhibit atrial $I_{Na}$, and terminate acute episodes of

AF.[14,15,16] However, the mechanism by which ranolazine terminates acute AF remains poorly understood. Furthermore, very limited information is available about the action of ranolazine in persistent AF. Therefore, the main goal of this study was to determine the effects of ranolazine and examine the underlying mechanisms in sheep models of paroxysmal and persistent AF (PxAF and PsAF, respectively).

We studied the dynamics of AF in isolated sheep hearts in the absence and presence of ranolazine by analyzing rotor properties such as dominant frequency (DF), wavebreaks or singularity points (SP), and rotor tip meander area and lifespan, as spiral waves have been shown to underlie the maintenance of AF.[17] Our results suggest that ranolazine abolishes reentry only in PxAF, and this can be explained in part by the different effects of the drug on rotor dynamics in PxAF versus PsAF.

**Methods**

The data, analytic methods, and study materials will not be made available to other researchers for purposes of reproducing the results or replicating the procedure.

Male sheep weighing 30–40 kg were used in the study. The animal protocol was approved by the University Committee on Use and Care of Animals of the University of Michigan and conforms to the Guide for Care and Use of Laboratory Animals by the United States National Institutes of Health. Sheep hearts were isolated and Langendorff-perfused as described previously.[8,18,19] The PsAF sheep model was generated using intermittent atrial tachypacing, and the PxAF model of AF was generated using acute stretch, as described in previous studies.[7,8,18,19] The effects of ranolazine were evaluated in both PxAF and PsAF models.

PxAF model: To increase AF susceptibility in isolated hearts from healthy sheep, we maintained intra-atrial pressure at 15 cm$H_2O$ (stretch-induced PxAF) throughout the experiment. We induced AF by burst atrial pacing at cycle lengths between 100–150 ms. Baseline AF remained stable for 30 minutes before application of ranolazine.

PsAF model: Sustained atrial tachypacing (20 Hz) was used to establish PsAF in sheep,[7,8] after which hearts were isolated and used for studying AF dynamics using optical imaging. *Surgical procedures for PsAF induction:* Dual chamber pacemaker implantations were performed under general anesthesia. Sheep were sedated with intramuscular injections of buprenorphine (0.005−0.01 mg/kg) and xylazine (0.2 mg/kg). Propofol (4−6 mg/kg) was given intravenously for anesthesia induction and maintained with inhaled isoflurane (1−2%). Animals were intubated and artificially ventilated via endotracheal tube. A bipolar, single-lead pacing electrode (St. Jude, MN, USA) was introduced via right jugular vein, directed to right atrial appendage (RAA) under fluoroscopy, and connected to a pacemaker canister (St Jude, MN, USA) inserted subcutaneously in the neck. An implantable loop recorder (ILR, Medtronic Reveal XT® Insertable Cardiac Monitor, MN, USA) was also positioned in a parasternal subcutaneous pouch near the left atrium to monitor heart rhythm. *Pacing protocol:* Animals were paced at 20 Hz for 30 seconds followed by a ≥10 second sensing period before pacing was resumed if sinus rhythm was detected. Pacing was maintained for an average of 24 weeks before *ex vivo* experiments. Pacemakers and ILRs were interrogated weekly. *Ex vivo* experiments were conducted once each animal had achieved at least 7 days of uninterrupted persistent AF.

Langendorff setup and optical mapping: Sheep hearts were removed via sternotomy (from either healthy sheep for PxAF or atrially-tachypaced sheep for PsAF), cannulated through the aorta, and connected to a Langendorff-perfusion system with recirculating oxygenated Tyrode's solution at a flow rate of 200–240 mL/min (pH 7.4, 35.5–37.5°C). The composition of the

Tyrode's solution was (mM): NaCl 130, KCl 4, $MgCl_2$ 1, $CaCl_2$ 1.8, $NaHCO_3$ 24, $NaH_2PO_4$ 1.2, glucose 5.6 and albumin 0.04 g/L. We used blebbistatin (10–20 μM, Enzo Life Science, NY, USA) to minimize motion artifact during optical mapping. After atrial transseptal puncture to equilibrate left and right atrial pressures, we ligated all vein orifices except the inferior vena cava which we cannulated with an outflow tube connected to a pressure transducer. Intra-atrial pressure was calibrated and controlled by adjusting the height of the outflow tube. We administered a 5–15 mL bolus injection of the voltage-sensitive di-4-ANEPPS (10 mg/mL, Sigma-Aldrich Co., St Louis, MO, USA), and then mapped the left atrial epicardium ($LA_{epi}$) and endocardial posterior left atrium ($PLA_{endo}$) simultaneously, as described previously.[7,8,18,19] We used a CCD video camera (80x80 pixels, 600 frames/second) to capture emitted fluorescence from the epicardial LA surface. We used a second CCD camera coupled to a rigid borescope through a custom-made eyepiece adapter, and introduced the borescope through the anterior LV base, across the mitral valve, focusing on the endocardial PLA surface. We maintained intra-atrial pressure at 5 $cmH_2O$ throughout experiments in PsAF animals to mimic normal diastolic LA pressure. In stretch-induced PxAF we increased intra-atrial pressure to 15 $cmH_2O$. After inducing AF by burst atrial pacing, we ensured baseline AF characteristics in PxAF and PsAF were stable for 30 minutes before adding ranolazine to the perfusate, and acquired five-second movies at 2-minute intervals. We calculated dominant frequency (DF) using Fast Fourier Transform of time-series fluorescence signals at each pixel, and constructed DF maps for each optical movie.

Pharmacological protocols: We assessed the effects of 10 μM ranolazine (Sigma-Aldrich Co., MO, USA) dissolved in non-recirculating Tyrode's solution; the concentration of ranolazine used was selected partly based on earlier studies.[14] This concentration is in the upper range of values observed in patients taking a maximum recommended dose of 1000 mg twice daily,

producing a mean steady-state plasma concentration of 6 μM (95% confidence interval: 1 –14 μM; based on Ranexa prescribing information, Gilead Sciences, Inc.). Drug perfusion was maintained for 20 minutes. In a separate set of experiments carried out in PsAF sheep hearts, the concentration of ranolazine was doubled (20 μM) after 20 minutes and maintained for another 20 minutes, followed by addition of dofetilide (1 μM) to the perfusate.

Computer simulations: We simulated reentry in a 2D rectangular sheet (6cm×6cm, or 600×600 cells) using our ionic model of the human atrial action potential[20] to provide insights into experimental results. Numerical techniques were similar to those used previously.[7,8,21,22] We modified the ionic model to introduce electrical remodeling as observed in AF,[7] and sustained rotors were induced via cross-field stimulation. A small rectangular block of cells was made unexcitable by eliminating their connections with neighboring cells to simulate a line of conduction block representing fibrosis. The effects of ranolazine were mimicked by decreasing the maximal conductance of peak $I_{Na}$.

Data analyses: Optical mapping data were analyzed using custom software (SCROLL, Dr. Sergey Mironov) as previously.[8,18,19] Analyses included maximal DF, SP density, rotor core trajectory area and lifespan (mean time of rotor existence), as well as AF cycle length (AFCL). For these analyses a rotor was defined as completion of at least one full rotation.

Statistical analysis: Statistical analyses were performed using GraphPad Prism 7. Continuous variables with normal distributions were expressed as mean±SEM. Normality of each data set was assessed by a Shapiro-Wilk test and QQ plot, and equality of variance was assessed by F-test. For non-normal data, the nonparametric Wilcoxon signed-rank test was performed for comparison of means. Comparisons of drug effects with baseline values were performed using paired t-tests or one-way repeated measures ANOVA where appropriate. A value of $p<0.05$ was considered statistically significant.

## Results

*Ex-vivo AF experiments*

The anti-AF properties of ranolazine were studied using optical mapping of atrial electrical activity in Langendorff-perfused sheep hearts. Sustained AF for >30 minutes is uncommon in healthy sheep; therefore, we used a model of stretch-induced AF[18] to determine drug effects in PxAF. PsAF was studied in perfused hearts isolated from chronic atrially tachypaced animals.[7,8]

*Ranolazine effects on stretch-induced paroxysmal AF*

After increasing intra-atrial pressure from 5 to 15 $cmH_2O$, AF was easily induced by burst atrial pacing. The baseline phase of the protocol consisted of simultaneous optical mapping of endocardial PLA and epicardial LA during PxAF for >30 min. During baseline, DF in $LA_{epi}$ reached an average of 8.3±0.4 Hz (Figure 1, *N*=8). Maximal DF in $PLA_{endo}$ reached 10.6±0.8 Hz at the end of baseline self-sustained AF (Supplemental Figure S1; *N*=8). After 30 minutes of baseline AF recordings, 10 μM ranolazine was added to the perfusate without recirculation. In the presence of ranolazine, DF decreased in all hearts in both $LA_{epi}$ and $PLA_{endo}$. Representative examples of DF maps in $LA_{epi}$ before and after ranolazine (10 μM) are shown in Figure 1A. After an average of 14.9±2.0 min of application of ranolazine (range: 6–20 min), stretch-induced PxAF converted to SR in all hearts (Figure 1B). Average maximal DF in $LA_{epi}$ just prior to termination of AF decreased significantly to 6.2±0.5 Hz ($p$<0.01) compared to baseline (Figure 1C).

The number of wavebreaks during AF was analyzed before and after ranolazine perfusion by quantifying the density of singularity points (SP) in phase maps.[23] Figure 2A shows representative phase movie snapshots displaying multiple SPs before (left) and during (right)

application of 10 μM ranolazine. In each experiment, SP density (normalized over area and time) decreased in $LA_{epi}$ during perfusion of ranolazine (Figure 2B). As shown in Figure 2C, on average, perfusion of ranolazine reduced SP density from a baseline of 0.070±0.007 to 0.039±0.005 $cm^{-2}s^{-1}$ just prior to AF termination ($p$<0.001).

Density of SPs could not be similarly quantified in $PLA_{endo}$ because the borescope viewing area could not be calibrated accurately (endocardial wide-angle lens distortion). However, effects of ranolazine on DF and SP density in PLA endocardium were qualitatively like those on the epicardium (Supplemental Figure S1 C-D).

To analyze AF dynamics further, we identified rotors with at least one complete rotation and measured the area within the rotor tip trajectory and rotor lifespans (Figure 3). During stretch-induced PxAF, there was no significant difference between these rotor characteristics on the $LA_{epi}$ before or during perfusion with ranolazine. Rotor trajectory areas were 30.2±5.7 $mm^2$ and 36.1±9.1 $mm^2$ (p=n.s.) before and during perfusion with ranolazine, respectively. Likewise, rotor lifespan before and during the perfusion with ranolazine measured 0.50±0.09 s and 0.56±0.11 s, respectively (p=n.s.). Similar effects were observed in $PLA_{endo}$ (Supplemental Figure S2). Thus, termination of stretch-induced PxAF by ranolazine was associated with a decrease in both maximal DF and SP density, without affecting the average area within the rotor trajectory or rotor lifespan.

*Ranolazine effects on persistent AF*

Nine hearts were isolated from chronically tachypaced animals after PsAF had been maintained for at least 7 days to investigate arrhythmia dynamics and potential antiarrhythmic effects of ranolazine. Intra-atrial pressure was maintained at a physiologic level of 5 $cmH_2O$. AF was induced by pacing and sustained for at least 30 minutes. Representative examples of DF maps in $LA_{epi}$ from PsAF sheep hearts before and during perfusion with ranolazine (10 μM) are shown

in Figure 4A. Similar to stretch-induced PxAF, in $LA_{epi}$ ranolazine reduced maximum DF in all hearts (Figure 4B). Prior to application of ranolazine to the perfusate, the average baseline value of maximum DF in $LA_{epi}$ was 8.3±0.5 Hz, which was slightly slower than in $PLA_{endo}$ (9.6±0.8 Hz, Supplemental Figure 3B). In the continuous presence of 10 μM ranolazine there was a rapid decrease in the maximum DF to 6.5±0.4 Hz within 10 minutes ($p$<0.01, Figure 4C). However, unlike in the stretch-induced PxAF model, PsAF was not terminated in any heart ($N$=9) after up to 20 minutes of perfusion with ranolazine.

Figure 5A shows typical phase movie snapshots during PsAF with SPs before (left) and during (right) perfusion with ranolazine on $LA_{epi}$, and representative time courses of SP density are shown in Figure 5B. Unlike PxAF, perfusion with 10 μM ranolazine did not significantly modify average SP density during PsAF (Figure 5C). Average SP density before and during ranolazine perfusion was 0.048±0.011 and 0.043±0.016 $cm^{-2}s^{-1}$ respectively ($p$=n.s.). In contrast to stretch-induced PxAF, average rotor trajectory areas and lifespans were significantly increased in $LA_{epi}$ during perfusion with ranolazine in hearts from PsAF sheep (Figure 6). Rotor trajectory areas were 38.0±7.0 $mm^2$ and 65.0±12.9 $mm^2$ ($p$<0.02), respectively before and during perfusion with ranolazine, while rotor lifespans were 0.49±0.07 s and 1.01±0.19 s ($p$<0.05), respectively before and during perfusion with ranolazine. Similar effects were observed in the $PLA_{endo}$ (Supplemental Figure 4).

The differential effects of ranolazine on stretch-induced PxAF versus tachypacing-induced PsAF suggested potentially different substrates for arrhythmia maintenance, despite similar maximum DF values at baseline and during application of ranolazine. The SP density during baseline AF was greater in PxAF than PsAF (Supplemental Figure 5). Thus, we compared the effects of ranolazine on AFCL distribution in time and space in both PxAF and PsAF using an automated algorithm to measure times between consecutive voltage nadirs during each movie frame

across all pixels (Figure 7A-D). Distributions of AFCL were unimodal (negative skew) and the average peak AFCL at baseline was similar between PxAF and PsAF (135.2±5.5 ms and 134.5±11.1 ms, respectively; *p*=n.s.; Figure 7E). In the presence of ranolazine, AFCL was significantly prolonged to 181.7±9.9 ms ($p<0.001$) in PxAF and to 168.6±13.1 ms ($p<0.002$) in PsAF. To assess the effects of ranolazine on AFCL distribution we quantified variance in AFCL by measuring full width at half maximum (FWHM) of AFCL distribution curves (Figure 7F); while baseline values were not significantly different between PxAF and PsAF ($p=0.08$), ranolazine increased AFCL-FWHM only in PsAF, likely reflecting increases in the spatio-temporal dispersion of both APD and effective refractory period (ERP), with no change observed in PxAF.

In a separate series of experiments in tachypaced PsAF sheep ($N=5$), we further investigated whether increasing the concentration of ranolazine (from 10 to 20 μM), or addition of another antiarrhythmic drug, dofetilide (1 μM) would affect PsAF (Figure 8A). After 30 minutes of baseline PsAF, average DF was 8.6±0.4 Hz. Ranolazine (10 μM) was then added to the perfusate causing a significant decrease in average maximal DF compared to the end of baseline ($p<0.05$), reaching an average minimum of 6.9±0.6 Hz. After 15 minutes, the ranolazine concentration in the perfusate was increased to 20 μM. Average maximal DF was not significantly different from average maximal DF at the lower dose, reaching the mean lowest value of 7.2±0.5 Hz, and PsAF continued in all hearts. Lastly, dofetilide (1 μM) was added to the perfusate in the continuous presence of 20 μM ranolazine. With the addition of dofetilide, maximal DF reached an average lowest value of 6.6±0.8 Hz, still significantly lower than baseline ($p<0.05$), but not different than with either concentration of ranolazine alone. While each treatment resulted in a lower DF on the $LA_{epi}$ compared to baseline (Figure 8A), PsAF was not terminated with addition of dofetilide. Likewise, density of SPs was not affected by either the increased dose of ranolazine or addition of dofetilide (Figure 8B). SP density measured

0.093±0.021 $cm^{-2}s^{-1}$ at the end of baseline, decreased to a minimum of 0.058±0.020 $cm^{-2}s^{-1}$ with 10 μM ranolazine ($p$=0.11 versus baseline), 0.064±0.020 $cm^{-2}s^{-1}$ with 20 μM ranolazine ($p$=0.059 versus baseline), and 0.082±0.021 $cm^{-2}s^{-1}$ with 20 μM ranolazine plus 1 μM dofetilide ($p$=0.082 versus baseline). Notably, hearts from these sheep came from five animals that had briefly received prior treatments (one animal had a 2-week regimen of eplerenone, a mineralocorticoid receptor antagonist; and the other four had previously received the galectin-3 inhibitor, GM-CT-01); however, all treatments were discontinued at least eight weeks prior to the terminal optical mapping study, during which, intermittent tachypacing continued as the animals progressed to self-sustained PsAF.

Numerical predictions: why ranolazine does not reduce SP density in PsAF

We conducted numerical simulations to obtain additional insights into our experimental findings. Stable rotors were induced in simulated 2D tissue sheets for 4 seconds, incorporating properties of ionic remodeling observed in AF. Simulated AF produced rotors with a maximal DF of 9.5 Hz and a tip trajectory spanning a relatively small area (Supplemental Figure S6, left panels). To mimic the effects of ranolazine, maximal conductance of $I_{Na}$ was reduced by 42%, which decreased tissue excitability. The simulated effects of ranolazine slowed maximal rotor frequency to 3.0 Hz, and substantially increased meander area of the tip trajectory (Supplemental Figure S6, right panels). These simulations mimic properties of rotors observed in persistent AF experiments. Additional decreases in $I_{Na}$ conductance did not allow for sustained rotors. We further analyzed the interaction of rotors with an unexcitable obstacle, which may be seen as functional or anatomical (white rectangles in Supplemental Figure S6). Under control AF conditions, the wave front emanating from the rotor fully circumnavigated the unexcitable obstacle without detachment (Supplemental Figure S6C, left). In contrast, when excitability was reduced to simulate effects of ranolazine, the wave front detached from the

distal side of the obstacle, creating a pair of new SPs and figure-8 reentrant wavelets (Supplemental Figure S6C, right). Thus, under conditions of reduced excitability, the interaction between rotor wavefronts and unexcitable obstacles reproduced the phenomenon of vortex shedding, as shown in previous simulation and experimental studies.[24]

## Discussion

The main novel findings from our study are as follows. Ranolazine reduces DF and SP density, and prolongs AFCL in PxAF. In contrast, in PsAF ranolazine reduces DF but not SP density, and prolongs AFCL, but variation in AFCL distribution is increased. These differences in spiral wave dynamics may reflect ranolazine-induced conduction slowing and spatial dispersion of refractoriness partly underlying the different outcomes in PxAF versus PsAF models in the presence of ranolazine. The potential underlying mechanisms are discussed below.

### Previous studies investigating antiarrhythmic drugs in AF cardioversion

Nattel and colleagues postulated that flecainide could terminate vagally-induced AF in the canine heart, because it increased wavelength (WL) during reentry.[25] They also showed that flecainide reduced regional differences and heterogeneities in WL and ERP.[25] Allessie and collaborators examined the effects of drugs in their goat model of AF;[11,26,27] however, they were unable to explain the pharmacological conversion of AF to sinus rhythm by a prolongation of WL.[26,27] Conversion of AF to SR could not be correlated with any other parameters such as AFCL, ERP, or conduction velocity, and they suggested that a widening of the temporal excitable gap could explain termination of AF in their experimental model.[27] Allessie's group also examined the effects of antiarrhythmic drugs on sustained and long-duration AF, and found that their efficacy to terminate AF decreased with time.[11] They postulated that the failure of

antiarrhythmic drugs to terminate AF was related to an increase in the critical AFCL required for successful pharmacological cardioversion. Studies have also explored the action of ranolazine, in a stretch model of acute AF in rabbits.[16] The effect of ranolazine to prolong ERP, inter-atrial conduction time, and post-repolarization-refractoriness (PRR) was invoked to explain the reduced inducibility of AF in that study.[16] A recent report indicated that the synthetic compound pentamidine analogue 6 (PA-6) was able to cardiovert persistent AF to SR in the goat model (developed with 3 weeks of atrial tachypacing), and this was attributed to an increase in AFCL and decrease in AF complexity (number of fibrillation waves); the primary ionic target of PA-6 was indicated to be the inward rectifier potassium current, $I_{K1}$.[39]

Explaining the actions of drugs in AF based on spiral wave properties

Recent data suggest that rotors may underlie the maintenance of AF in animal models and humans.[17,28] Therefore, studying the effects of drugs on rotors may provide insights into their antiarrhythmic mechanisms. Filguerias-Rama and colleagues studied the effects of chloroquine and flecainide on the maintenance of AF during continuous stretch applied to the atria in isolated sheep hearts.[18] They found that chloroquine was more effective in terminating stretch-induced AF compared to flecainide (which failed to convert to SR in any experiment), in part by increasing core size and reducing DF.[18] More recently, Takemoto et al[36] extended the chloroquine studies to the PsAF model of sheep, similar to the one used in our studies. In all isolated heart experiments, chloroquine was able to terminate PsAF, by significantly reducing DF, and similar results were observed with tertiapin; however, the effects of these drugs on SP density were not investigated.[36] Patch clamp experiments in single cells and molecular simulation studies show that chloroquine is a highly effective blocker of inward rectifier $K^+$ channels, including $I_{K1}$[37] and the constitutively active acetylcholine-activated $K^+$ current, $I_{KACh}$.[2,36]

Therefore, we sought to quantify the effects of ranolazine on dynamic properties of rotors. Our results show that ranolazine reduces DF in both PxAF and PsAF. This suggests that the effect of ranolazine to interact with $I_{Na}$ *per se* is unlikely to be impaired in either PxAF or PsAF. Moreover, our data reveal that ranolazine reduces SP (or wavebreak) density only in acute PxAF, but not in chronic PsAF. Rotor lifespans and trajectory areas were increased by ranolazine in PsAF, but unaffected in PxAF. Computational simulations show that when $I_{Na}$ density is decreased, rotor DF is concomitantly reduced as expected, whereas core meander is increased, consistent with the experimental data of reduced excitability. However, reduced excitability in the presence of a fixed anatomical obstacle in the simulations, representing fibrosis in PsAF, led to vortex shedding and creation of new rotors. This phenomenon provides one potential mechanism for the unchanged SP density which may also help sustain PsAF. AFCL heterogeneity was also increased in PsAF (but not PxAF), which may reflect increased ERP dispersion in both time and space contributing to rotor meandering, enhanced vortex shedding and rotor proliferation compensating for any rotor loss. The latter might help explain the inefficacy of ranolazine to terminate PsAF. Previous experimental studies have provided evidence of increased distribution in AFCL contributing to AF maintenance.[41] Clearly other possibilities exist, such as rotor attachment to obstacles (anchoring), or formation of anatomical reentry to sustain AF.[29] These latter phenomena were not observed during our experiments; however, our current imaging technology only maps parts of the atria, making it difficult to rule out this possibility in areas of the atria that were not mapped (such as the septum or perivalvular regions). However, structural remodeling of the atrium including fibrosis is not a necessary condition for maintenance of AF as shown in recent studies using eplerenone.[38] Although eplerenone mitigated fibrosis and atrial dilation in the chronically atrial-tachypaced sheep hearts, pacing-induced electrical remodeling was able to sustain persistent AF.[38]

Effects of ranolazine

The effect of ranolazine to convert AF to sinus rhythm is likely a result of preferential blockade of the open state of the sodium channel, yielding a use dependent effect on sodium current at faster activation rates, as occurs during AF.[42] One advantage of ranolazine over other sodium channel blockers is its atrial selectivity for inhibition of $I_{Na}$.[14] Sodium channel blockade by ranolazine is dependent on membrane potential and activation rate, and is much more potent in atria than ventricle.[14] Atrial and ventricular sodium channels have distinct biophysical inactivation properties, with a much more negative half-inactivation voltage ($V_{0.5}$) in atria than ventricles, differing by about 15 mV.[14] The presence of ranolazine negatively shifts the $V_{0.5}$ for sodium channel inactivation, but the shift is twice as large in atria than ventricles. These differences in inactivation biophysical properties, combined with a more depolarized diastolic membrane potential and slower phase 3 repolarization in atria, imparts greater $I_{Na}$ inhibition from ranolazine in atria than in ventricles. Despite its selectivity for $I_{Na}$, ranolazine may also exert its antiarrhythmic effects in part by blockade of other currents in a concentration dependent manner, notably, the rapid delayed rectifier $K^+$ current, $I_{Kr}$. Taken together, these ionic effects might help explain the conversion of PxAF to SR by ranolazine in our studies. The lack of effect of ranolazine in PsAF compared to success of chloroquine or PA-6 can also be partly attributed to the differences in key ionic targets of the respective drugs; ranolazine selectively tends to inhibit $I_{Na}$, whereas chloroquine/PA-6 target inward rectifier $K^+$ channels which have been shown to be key in maintaining rotors that drive fibrillation.[17] This is particularly relevant for PsAF, where the density of $I_{K1}$ is increased, both in the sheep model[7] and in humans.[40]

Significance of SP dynamics

Rotors are emerging as a central phenomenon in the mechanism of AF.[17] Rotors represent a form of functional reentrant activity, serving as the driving source, where the wavefront and wavetail meet and create a singularity point (SP) in phase space.[17] Rotors pivot around the SP, which can meander across tissue. On the surface of the endocardium or epicardium during AF, the rotor appears as a spiral wave circling around a SP at high speed, but the spiral represents merely a 2-dimensional boundary of a 3-dimensional scroll wave rotating around a filament that meets the surface at the SP.[17] Rotors can be triggered by multiple mechanisms including alternans, unidirectional block, and vortex shedding, as observed in our simulations. In the presence of ample excitable tissue, sustained reentry can be maintained; however, collision with another wave, anatomical boundary, or inexcitable region can lead to annihilation. Thus, SP density represents the net balance of rotor initiation and annihilation. Our rotor analysis focused on rotors that lasted at least one rotation, and revealed average rotor lifespans of 0.5 to 1 sec. In the case of PxAF, ranolazine decreased SP density but had no effect on rotor lifespan, suggesting that in the presence of ranolazine, rotor annihilation exceeded rotor initiation until termination of AF. On the other hand, in PsAF, ranolazine had no effect on SP density while mean rotor lifespan and AFCL dispersion increased, suggesting that rates of rotor initiation matched annihilation, while rotors lasted twice as long and meandered over a larger area. The computational results point to vortex shedding, secondary to reduced excitability in the presence of obstacles to wave propagation, as one of the mechanisms that can sustain rotor formation.

Limitations

Our experiments focused mainly on actions of ranolazine in AF that are related to rotors, and not focal activity.[5] The experimental results are pertinent to pacing-induced remodeling due to lone AF, and not more complex remodeling in the atria, such as in the case of heart failure.[5,30]

Our studies have focused on the effect of ranolazine in cardioverting AF in isolated sheep hearts, whereas previous studies in a canine heart failure model have examined the effect of ranolazine in preventing the initiation of AF.[30] These differences in animal models (sheep model of tachypaced AF versus canine model of heart failure, which can result in differences in electrical and structural remodeling) and AF mechanisms being studied (initiation versus termination) could in part explain the success of ranolazine in preventing AF recurrence in the canine heart failure model, compared to its failure in terminating sustained AF in our PsAF sheep hearts. Although ranolazine is not known to inhibit $I_{K1}$, it is not clear whether it can inhibit other inward rectifiers such as $I_{KACh}$, which has been shown to be important in sustaining PsAF in the sheep model.[36] In our simplified numerical simulations, we have not taken into account the complex geometry of atrial tissue, the impact of patchy versus interstitial fibrosis, or heterogeneity of electrical properties that may help sustain AF.[5] Furthermore, we simulated the effects of ranolazine by simple decreases in maximal conductance of $I_{Na}$, and have not considered the complex pharmacokinetics of sodium channel block[31] (use-dependence, tonic and phasic block, or peak versus late $I_{Na}$,[32]). Differences in post-repolarization refractoriness could also play a role in the varied effects of ranolazine in PxAF versus PsAF models, and at present it is not possible to directly correlate the SP density with post-repolarization refractoriness. While we have previously demonstrated that peak $I_{Na}$ is decreased in the PsAF model, the extent to which late $I_{Na}$ is changed in our AF model remains unknown. This, along with regulation of other $Ca^{2+}$ and $K^+$ channels leads to complex electrical remodeling in the sheep model of PsAF,[7,8] and may play a role in the observed actions of ranolazine, which requires further investigation. Other cellular actions of ranolazine, besides sodium channel blockade, such as $I_{Kr}$ inhibition may have also played a role in the observed effects on AF. In canine atrial[33] and ventricular[34] myocytes, ranolazine blocks $I_{Kr}$, the addition of dofetilide during perfusion with ranolazine was still unable to cardiovert PsAF. Recent experiments suggest a

role for epicardial-endocardial dyssynchrony in the maintenance of PsAF.[35] However, our experimental setup (inability to map transmurally, as well as to assess spatial dimensions on the posterior left atrial endocardium accurately) prevents us from testing this idea.

**Acknowledgements**

We thank Dr. Vedran Velagic and Danillo Souza for assistance with animal handling and data collection.

**Sources of Funding**

This work was supported by: grants from the NIH National Heart, Lung, and Blood Institute R01-HL118304 (O.B.) and R01-HL122352 (J.J.); the Leducq Foundation (J.J., O.B., S.V.P.); the University of Michigan Health System and Peking University Health Sciences Center Joint Institute for Translational and Clinical Research (J.J.); Ministerio de Economía y Competitividad and Fondo Europeo de Desarrollo Regional (FEDER) (J.J.); the JHRS fellowship program from Medtronic Japan, Uehara Memorial Foundation (Y.T.); American Heart Association postdoctoral fellowship (Y.T.); research grants from Gilead Sciences Inc (J.J., S.V.P.); and research support and assistance with implantable devices from St. Jude Medical and Medtronic Inc (J.J., O.B.).

**Disclosures and Disclaimer**

J.J. served as a consultant for Topera-Abbott Laboratories. O.B. is cofounder and Scientific Officer of Rhythm Solutions, Inc., Research and Development Director for S.A.S. Volta Medical and consultant to Acutus Medical. L.B. and S.R. were employees of Gilead Sciences Inc at the time of this study. This work was completed while S.V.P was working at the University of Michigan. S.V.P now works at the US Food and Drug Administration (FDA). This article reflects the views of the author (S.V.P), and should not be construed to represent the FDA's views or policies.

**References**


1. Khaji A, Kowey PR. Update on atrial fibrillation. *Trends Cardiovasc Med.* 2017;27(1):14-25.
2. Dobrev D, Nattel S. New antiarrhythmic drugs for treatment of atrial fibrillation. *Lancet.* 2010;375(9721):1212-1223.
3. Kannankeril P, Roden DM, Darbar D. Drug-induced long QT syndrome. *Pharmacol Rev.* 2010;62(4):760-781.
4. Heijman J, Voigt N, Nattel S, Dobrev D. Cellular and molecular electrophysiology of atrial fibrillation initiation, maintenance, and progression. *Circ Res.* 2014;114(9):1483-1499.
5. Schotten U, Verheule S, Kirchhof P, Goette A. Pathophysiological mechanisms of atrial fibrillation: a translational appraisal. *Physiol Rev.* 2011;91(1):265-325.
6. Wijffels MC, Kirchhof CJ, Dorland R, Allessie MA. Atrial fibrillation begets atrial fibrillation. A study in awake chronically instrumented goats. *Circulation.* 1995;92(7):1954-1968.
7. Martins RP, Kaur K, Hwang E, Ramirez RJ, Willis BC, Filgueiras-Rama D, Ennis SR, Takemoto Y, Ponce-Balbuena D, Zarzoso M, O'Connell RP, Musa H, Guerrero-Serna G, Avula UM, Swartz MF, Bhushal S, Deo M, Pandit SV, Berenfeld O, Jalife J. Dominant frequency increase rate predicts transition from paroxysmal to long-term persistent atrial fibrillation. *Circulation.* 2014;129(14):1472-1482.
8. Takemoto Y, Ramirez RJ, Yokokawa M, Kaur K, Ponce-Balbuena D, Sinno MC, Willis BC, Ghanbari H, Ennis SR, Guerrero-Serna G, Henzi BC, Latchamsetty R, Ramos-Mondragon R, Musa H, Martins RP, Pandit SV, Noujaim SF, Crawford T, Jongnarangsin K, Pelosi F, Bogun F, Chugh A, Berenfeld O, Morady F, Oral H, Jalife J. Galectin-3 Regulates Atrial Fibrillation Remodeling and Predicts Catheter Ablation Outcomes. *JACC Basic Transl Sci.* 2016;1(3):143-154.

9. Franz MR, Karasik PL, Li C, Moubarak J, Chavez M. Electrical remodeling of the human atrium: similar effects in patients with chronic atrial fibrillation and atrial flutter. *J Am Coll Cardiol.* 1997;30(7):1785-1792.
10. Xu J, Cui G, Esmailian F, Plunkett M, Marelli D, Ardehali A, Odim J, Laks H, Sen L. Atrial extracellular matrix remodeling and the maintenance of atrial fibrillation. *Circulation.* 2004;109:363–368.
11. Eijsbouts S, Ausma J, Blaauw Y, Schotten U, Duytschaever M, Allessie MA. Serial cardioversion by class IC Drugs during 4 months of persistent atrial fibrillation in the goat. *J Cardiovasc Electrophysiol.* 2006;17(6):648-654.
12. Mont L, Bisbal F, Hernández-Madrid A, Pérez-Castellano N, Viñolas X, Arenal A, Arribas F, Fernández-Lozano I, Bodegas A, Cobos A, Matía R, Pérez-Villacastín J, Guerra JM, Ávila P, López-Gil M, Castro V, Arana JI, Brugada J; SARA investigators. Catheter ablation vs. antiarrhythmic drug treatment of persistent atrial fibrillation: a multicentre, randomized, controlled trial (SARA study). *Eur Heart J.* 2014;35(8):501-507.
13. Ravens U, Poulet C, Wettwer E, Knaut M. Atrial selectivity of antiarrhythmic drugs. *J Physiol.* 2013;591(17):4087-4097.
14. Burashnikov A, Di Diego JM, Zygmunt AC, Belardinelli L, Antzelevitch C. Atrium-selective sodium channel block as a strategy for suppression of atrial fibrillation: differences in sodium channel inactivation between atria and ventricles and the role of ranolazine. *Circulation.* 2007;116(13):1449-1457.
15. Kumar K, Nearing BD, Carvas M, Nascimento BC, Acar M, Belardinelli L, Verrier RL. Ranolazine exerts potent effects on atrial electrical properties and abbreviates atrial fibrillation duration in the intact porcine heart. *J Cardiovasc Electrophysiol.* 2009;20(7):796-802.

16. Milberg P, Frommeyer G, Ghezelbash S, Rajamani S, Osada N, Razvan R, Belardinelli L, Breithardt G, Eckardt L. Sodium channel block by ranolazine in an experimental model of stretch-related atrial fibrillation: prolongation of interatrial conduction time and increase in post-repolarization refractoriness. *Europace.* 2013;15(5):761-769
17. Pandit SV, Jalife J. Rotors and the dynamics of cardiac fibrillation. *Circ Res.* 2013;112(5):849-862.
18. Filgueiras-Rama D, Martins RP, Mironov S, Yamazaki M, Calvo CJ, Ennis SR, Bandaru K, Noujaim SF, Kalifa J, Berenfeld O, Jalife J. Chloroquine terminates stretch-induced atrial fibrillation more effectively than flecainide in the sheep heart. *Circ Arrhythm Electrophysiol.* 2012;5(3):561-570.
19. Filgueiras-Rama D, Price NF, Martins RP, Yamazaki M, Avula UM, Kaur K, Kalifa J, Ennis SR, Hwang E, Devabhaktuni V, Jalife J, Berenfeld O. Long-term frequency gradients during persistent atrial fibrillation in sheep are associated with stable sources in the left atrium. *Circ Arrhythm Electrophysiol.* 2012;5(6):1160-1167.
20. Grandi E, Pandit SV, Voigt N, Workman AJ, Dobrev D, Jalife J, Bers DM. Human atrial action potential and $Ca^{2+}$ model: sinus rhythm and chronic atrial fibrillation. *Circ Res.* 2011;109(9):1055-1066.
21. Pandit SV, Berenfeld O, Anumonwo JM, Zaritski RM, Kneller J, Nattel S, Jalife J. Ionic determinants of functional reentry in a 2-D model of human atrial cells during simulated chronic atrial fibrillation. *Biophys J.* 2005;88(6):3806-3821.
22. Deo M, Ruan Y, Pandit SV, Shah K, Berenfeld O, Blaufox A, Cerrone M, Noujaim SF, Denegri M, Jalife J, Priori SG. KCNJ2 mutation in short QT syndrome 3 results in atrial fibrillation and ventricular proarrhythmia. *Proc Natl Acad Sci USA.* 2013;110(11):4291-4296.

23. Pandit SV, Warren M, Mironov S, Tolkacheva EG, Kalifa J, Berenfeld O, Jalife J. Mechanisms underlying the antifibrillatory action of hyperkalemia in Guinea pig hearts. *Biophys J.* 2010;98(10):2091-2101.
24. Cabo C, Pertsov AM, Davidenko JM, Baxter WT, Gray RA, Jalife J. Vortex shedding as a precursor of turbulent electrical activity in cardiac muscle. *Biophys J.* 1996;70(3):1105-1111.
25. Wang Z, Pagé P, Nattel S. Mechanism of flecainide's antiarrhythmic action in experimental atrial fibrillation. *Circ Res.* 1992;71(2):271-287.
26. Wijffels MC, Dorland R, Allessie MA. Pharmacologic cardioversion of chronic atrial fibrillation in the goat by class IA, IC, and III drugs: a comparison between hydroquinidine, cibenzoline, flecainide, and d-sotalol. *J Cardiovasc Electrophysiol.* 1999;10(2):178-193.
27. Wijffels MC, Dorland R, Mast F, Allessie MA. Widening of the excitable gap during pharmacological cardioversion of atrial fibrillation in the goat: effects of cibenzoline, hydroquinidine, flecainide, and d-sotalol. *Circulation.* 2000;102(2):260-267.
28. Narayan SM, Krummen DE, Rappel WJ. Clinical mapping approach to diagnose electrical rotors and focal impulse sources for human atrial fibrillation. *J Cardiovasc Electrophysiol.* 2012;23(5):447-454.
29. Gonzales MJ, Vincent KP, Rappel WJ, Narayan SM, McCulloch AD. Structural contributions to fibrillatory rotors in a patient-derived computational model of the atria. *Europace.* 2014;16(Suppl 4):iv3-iv10.
30. Burashnikov A, Di Diego JM, Barajas-Martinez H, Hu D, Cordeiro JM, Moise NS, Kornreich BG, Belardinelli L, Antzelevitch C. Ranolazine effectively suppresses atrial fibrillation in the setting of heart failure. *Circ Heart Fail.* 2014;7:627-633.
31. January CT, Makielski JC. Pharmacology of the Sodium channel. Cardiac Electrophysiology: From Cell to Bedside. 5th edition, Saunders. 2009. 169-174.

32. Sossalla S, Kallmeyer B, Wagner S, Mazur M, Maurer U, Toischer K, Schmitto JD, Seipelt R, Schondube FA, Hasenfuss G, Belardinelli L, Maier LS. Altered $Na^+$ currents in atrial fibrillation: Effects of ranolazine on arrhythmias and contractility in human atrial myocardium. *J Am Coll Cardiol.* 2010;55(21):2330-2342.
33. Schram G, Zhang L, Derakhchan K, Ehrlich JR, Belardinelli L, Nattel S. Ranolazine: Ion-channel-blocking actions and *in vivo* electrophysiological effects. *Br J Pharmacol.* 2004;142(8):1300-1308.
34. Antzelevitch C, Belardinelli L, Zygmunt AC, Burashnikov A, Di Diego JM, Fish JM, Cordeiro JM, Thomas G. Electrophysiological effects of ranolazine, a novel antianginal agent with antiarrhythmic properties. *Circulation.* 2004;110(8):904-910.
35. Eckstein J, Zeemering S, Linz D, Maesen B, Verheule S, van Hunnik A, Crijns H, Allessie MA, Schotten U. Transmural conduction is the predominant mechanism of breakthrough during atrial fibrillation: evidence from simultaneous endo-epicardial high density activation mapping. *Circ Arrhythm Electrophysiol.* 2013;6(2):334-341.
36. Takemoto Y, Slough DP, Meinke G, Katnik C, Graziano ZA, Chidipi B, Reiser M, Alhadidy MM, Ramirez R, Salvador-Montañés O, Ennis S, Guerrero-Serna G, Haburcak M, Diehl C, Cuevas J, Jalife J, Bohm A, Lin YS, Noujaim SF. Structural basis for the antiarrhythmic blockade of a potassium channel with a small molecule. FASEB J. 2018 Apr;32(4):1778-1793.
37. Noujaim SF, Stuckey JA, Ponce-Balbuena D, Ferrer-Villada T, López-Izquierdo A, Pandit SV, Sánchez-Chapula JA, Jalife J. Structural bases for the different anti-fibrillatory effects of chloroquine and quinidine. Cardiovasc Res. 2011 Mar 1;89(4):862-9.
38. Takemoto Y, Ramirez RJ, Kaur K, Salvador-Montañés O, Ponce-Balbuena D, Ramos-Mondragón R, Ennis SR, Guerrero-Serna G, Berenfeld O, Jalife J. Eplerenone Reduces

Atrial Fibrillation Burden Without Preventing Atrial Electrical Remodeling. J Am Coll Cardiol. 2017 Dec 12;70(23):2893-2905.

39. Ji Y, Varkevisser R, Opacic D, Bossu A, Kuiper M, Beekman JDM, Yang S, Khan AP, Dobrev D, Voigt N, Wang MZ, Verheule S, Vos MA, van der Heyden MAG. The inward rectifier current inhibitor PA-6 terminates atrial fibrillation and does not cause ventricular arrhythmias in goat and dog models. Br J Pharmacol. 2017 Aug;174(15):2576-2590.
40. Workman AJ, Kane KA, Rankin AC. Cellular bases for human atrial fibrillation. Heart Rhythm. 2008 Jun;5(6 Suppl):S1-6.
41. Gaspo R, Bosch RF, Talajic M, Nattel S. Functional mechanisms underlying tachycardia-induced sustained atrial fibrillation in a chronic dog model. Circulation. 1997 Dec 2;96(11):4027-35.
42. Zygmunt AC, Nesterenko VV, Rajamani S, Hu D, Barajas-Martinez H, Belardinelli L, Antzelevitch C. Mechanisms of atrial-selective block of $Na^+$ channels by ranolazine: I. Experimental analysis of the use-dependent block. Am J Physiol: Heart Circ Physiol. 2011;301(4):H1606-H1614.

## Figure Legends

### Figure 1

**Effect of ranolazine on DF in stretch-induced paroxysmal AF on the LA epicardium from perfused hearts. (A)** Time course of maximal dominant frequency (DF) during paroxysmal AF in 8 sheep hearts. Continuous ranolazine perfusion begins at time 0 (dashed line). In all experiments, PxAF spontaneously converted to sinus rhythm within 20 minutes of ranolazine perfusion. **(B)** Average DF was significantly decreased during ranolazine perfusion (*$p$<0.01). **(C)** Representative DF maps of the LA epicardium before (left) and during (right) perfusion of ranolazine.

### Figure 2

**Effect of ranolazine on singularity point (SP) density in stretch-induced paroxysmal AF on the LA epicardium from perfused hearts. (A)** Time course of SP density during paroxysmal AF. At time=0 mins (dashed line) 10 μM ranolazine is added to the perfusate. **(B)** Average SP density was decreased (*$p$<0.001, $N$=8) during ranolazine perfusion. **(C)** Representative phase maps of the LA epicardium before (left) and during (right) perfusion of ranolazine show multiple rotors (white arrows indicate direction of rotation around SP).

### Figure 3

**Effect of ranolazine on rotor trajectory area and rotor lifespan in LA epicardium during stretch-induced paroxysmal AF. (A)** Rotor trajectory areas and **(B)** rotor lifespans were not significantly changed from baseline during ranolazine perfusion.

**Figure 4**

**Effect of ranolazine on DF in tachypacing-induced persistent AF on the LA epicardium from perfused hearts. (A)** Time course of maximal dominant frequency (DF) during persistent AF in 9 sheep hearts. Continuous ranolazine perfusion (10 μM) begins at time 0 (dashed line). **(B)** Average DF was decreased during ranolazine perfusion (**p*<0.01). **(C)** Representative DF maps of the LA epicardium before (left) and during (right) perfusion of ranolazine.

**Figure 5**

**Effect of ranolazine on singularity point (SP) density in tachypacing-induced persistent AF on the LA epicardium from perfused hearts. (A)** Time course of SP density during persistent AF in 9 sheep hearts. Continuous ranolazine (10 μM) perfusion begins at time 0 (dashed line). **(B)** Average SP density was not changed before and during perfusion of ranolazine. **(C)** Representative phase maps of the LA epicardium before (left) and during (right) perfusion of ranolazine show multiple rotors (white arrows indicate direction of rotation around SP).

**Figure 6**

**Effect of ranolazine on rotor trajectory area and rotor lifespan on the LA epicardium from perfused hearts in tachypacing-induced persistent AF. (A)** Rotor trajectory areas significantly increased in the presence of ranolazine. **(B)** Rotor lifespans were significantly prolonged during ranolazine perfusion (* *p*<0.05).

**Figure 7**

**AF cycle length (AFCL) during stretch-induced paroxysmal (Px) and tachypacing-induced persistent (Ps) AF. (A)** Representative phase map during PsAF. **(B)** Representative single-pixel optical voltage recording during PsAF displaying automated detection of upstroke (red)

and downstroke (green). AFCL is measured for each activation between consecutive nadirs (arrow in inset). For each movie frame a histogram is constructed to measure AFCL distribution. **(C)** All histograms from a movie are stacked vertically into 3D histograms with brighter colours representing count numbers. Left and right panels show representative stacked histograms of PsAF before and during application of ranolazine, respectively. For each movie, stacked histograms are averaged across all frames. **(D)** Representative average AFCL histograms from the same heart in PsAF before (black) and during (red) application of ranolazine show prolongation of mean and mode AFCL with ranolazine. **(E)** Quantification of AFCL shows ranolazine prolonged AFCL in both PxAF and PsAF. **(F)** Quantification of full width at half maximum (FWHM) as an index of variance of average AFCL histograms (lines indicate mean±SEM).

**Figure 8**

**Effects of ranolazine and dofetilide in persistent AF. (A)** In hearts from 5 sheep with tachypacing-induced persistent AF, after at least 30 minutes of baseline AF, 10 μM ranolazine was added to the perfusate for 15 minutes, followed by an increase in ranolazine concentration to 20 μM for 15 minutes, and lastly the addition of dofetilide (1 μM). The addition of dofetilide to ranolazine (20 μM) did not terminate persistent AF in any of the hearts, despite decreasing average DF on the LA epicardium (* $p<0.05$ versus end of baseline). **(B)** The higher concentration of ranolazine plus dofetilide did not significantly change average SP frequency on the LA epicardium ($p$=n.s. versus end of baseline).

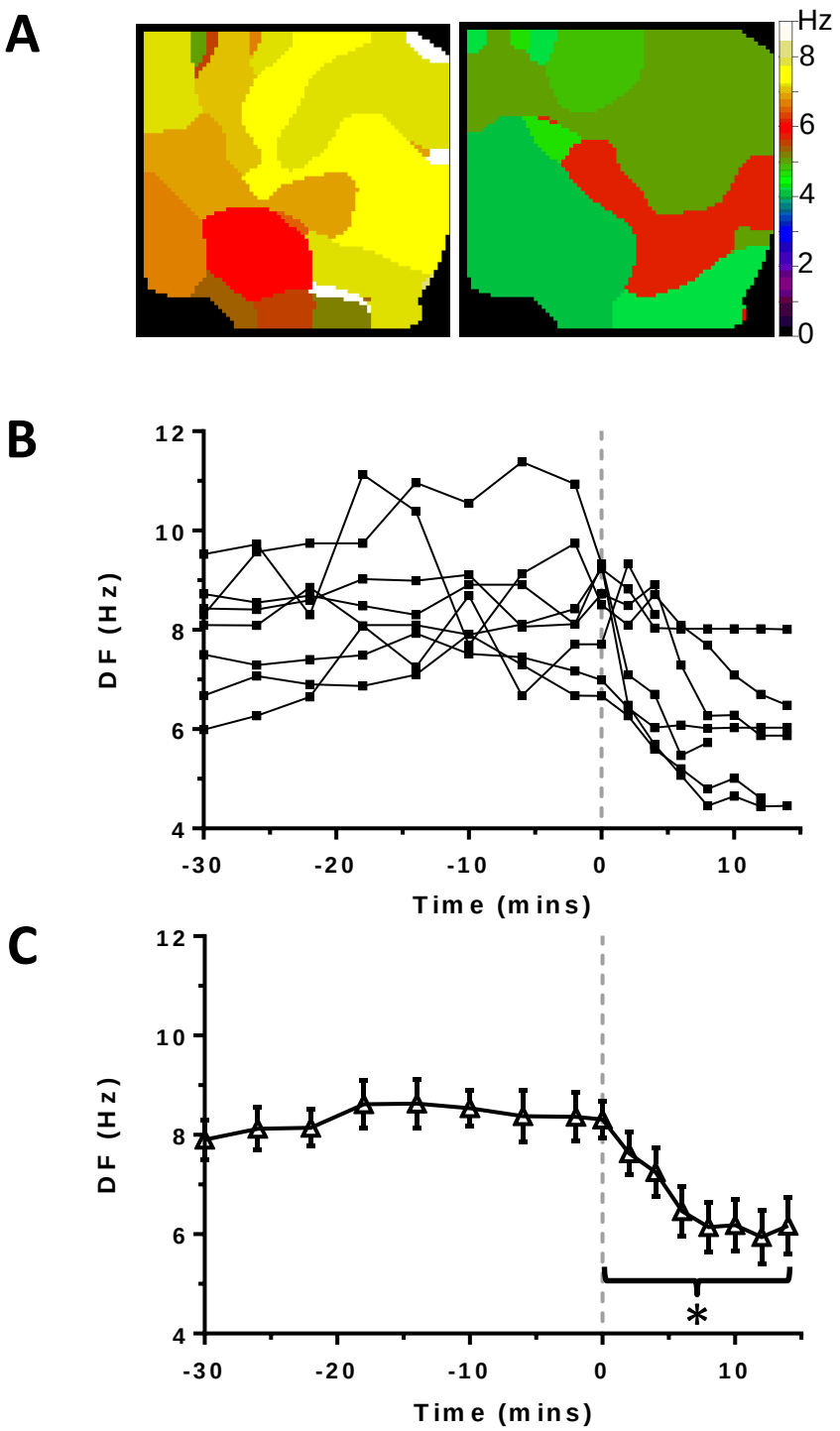


**Figure 1. Effect of ranolazine on DF in stretch-induced paroxysmal AF on the LA epicardium from perfused hearts. (A)** Representative DF maps of the LA epicardium before (left) and during (right) perfusion of ranolazine. **(B)** Time course of maximum dominant frequency (DF) during paroxysmal AF in 8 sheep hearts. Continuous perfusion with ranolazine begins at time 0 (dashed line). In all experiments, PxAF converted to sinus rhythm within 20 minutes of application of ranolazine. **(C)** Average DF is significantly decreased during perfusion with ranolazine (*****$p$<0.01).

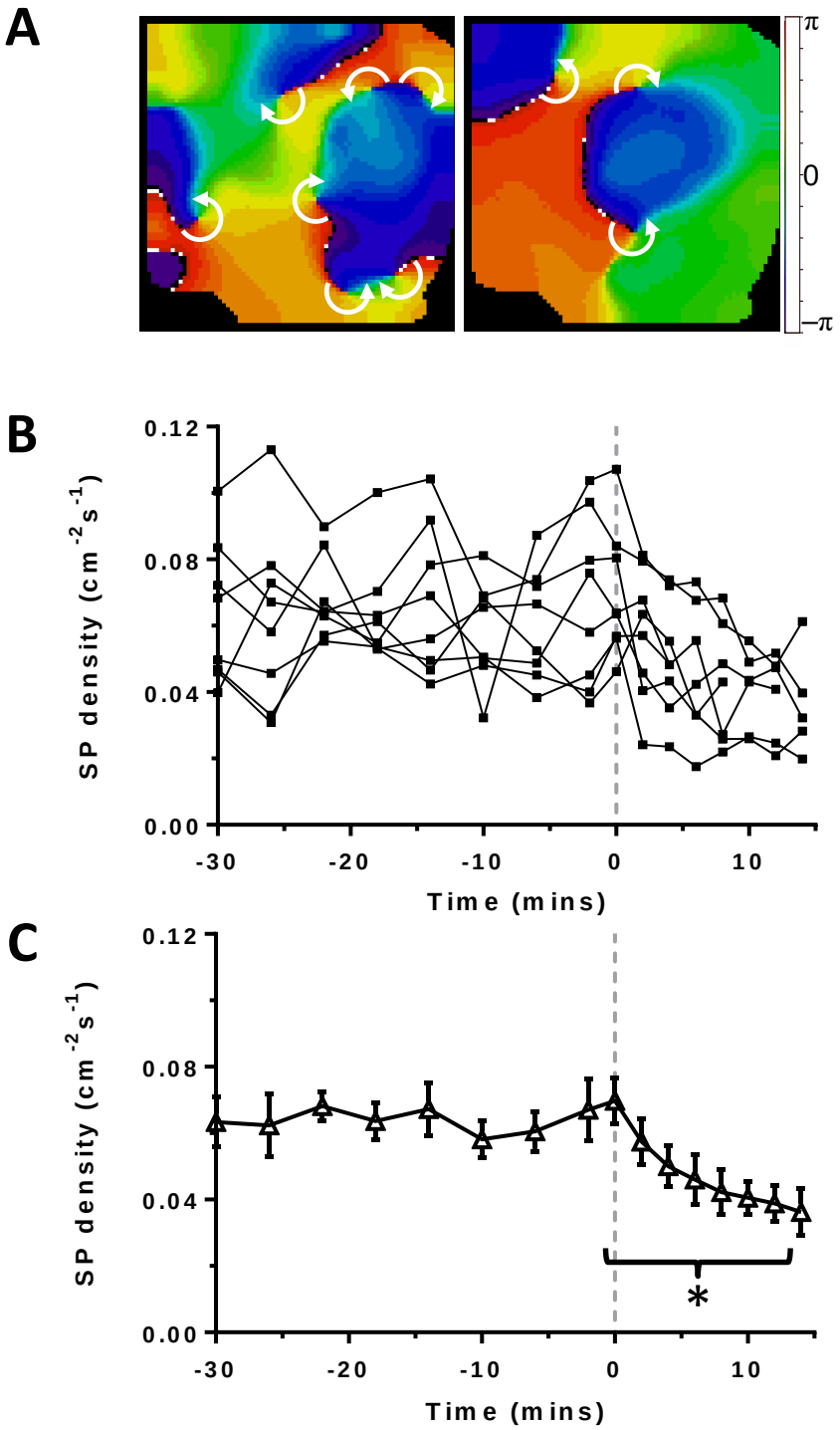


**Figure 2. Effect of ranolazine on singularity point (SP) density in stretch-induced paroxysmal AF on the LA epicardium from perfused hearts. (A)** Representative phase maps of the LA epicardium before (left) and during (right) perfusion with ranolazine shows multiple rotors (white arrows indicate direction of rotation around SP). **(B)** Time course of SP density during paroxysmal AF. At time 0 (dashed line) 10 µM ranolazine is added to the perfusate. **(C)** Average SP density is decreased (**p*<0.001, *N*=8) during perfusion with ranolazine.

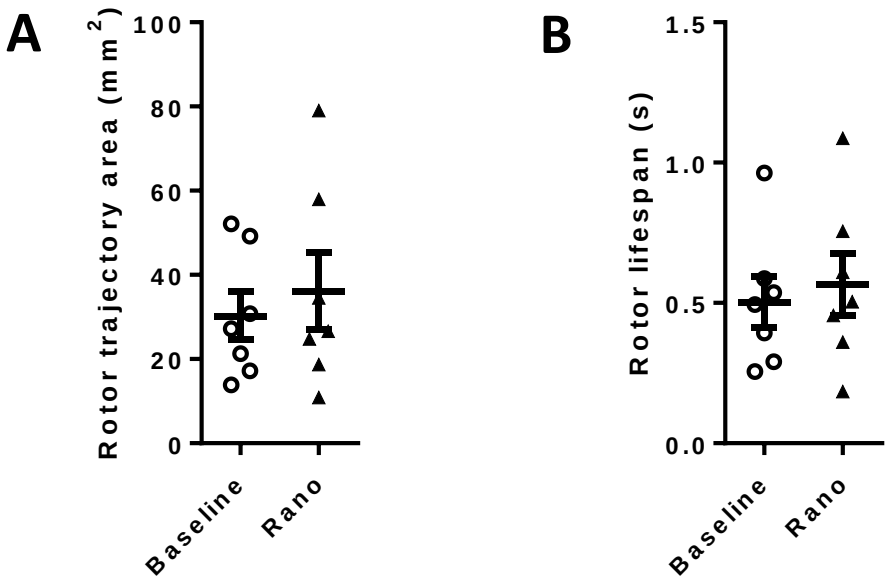


**Figure 3. Effect of ranolazine on rotor trajectory area and rotor lifespan in LA epicardium during stretch-induced paroxysmal AF. (A)** Rotor trajectory areas and **(B)** rotor lifespans were not significantly changed from baseline to after addition of ranolazine to the perfusate.

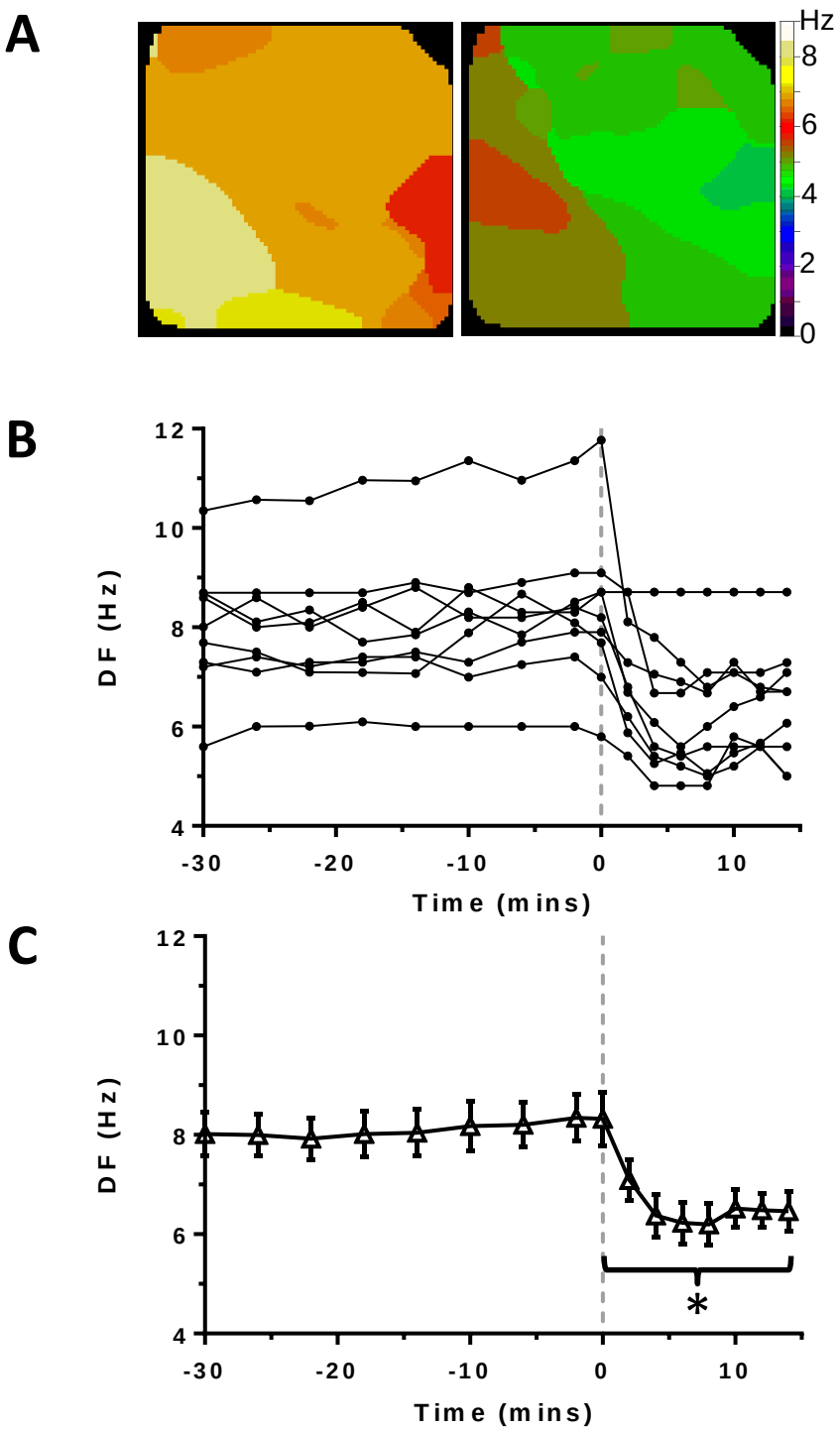


**Figure 4. Effect of ranolazine on DF in tachypacing-induced persistent AF on the LA epicardium from perfused hearts. (A)** Representative DF maps of the LA epicardium before (left) and during (right) perfusion with ranolazine. **(B)** Time course of maximum dominant frequency (DF) during persistent AF in 9 sheep hearts. Continuous perfusion with ranolazine (10 µM) begins at time 0 (dashed line). **(C)** Average DF is decreased during perfusion with ranolazine (*$p$<0.01).

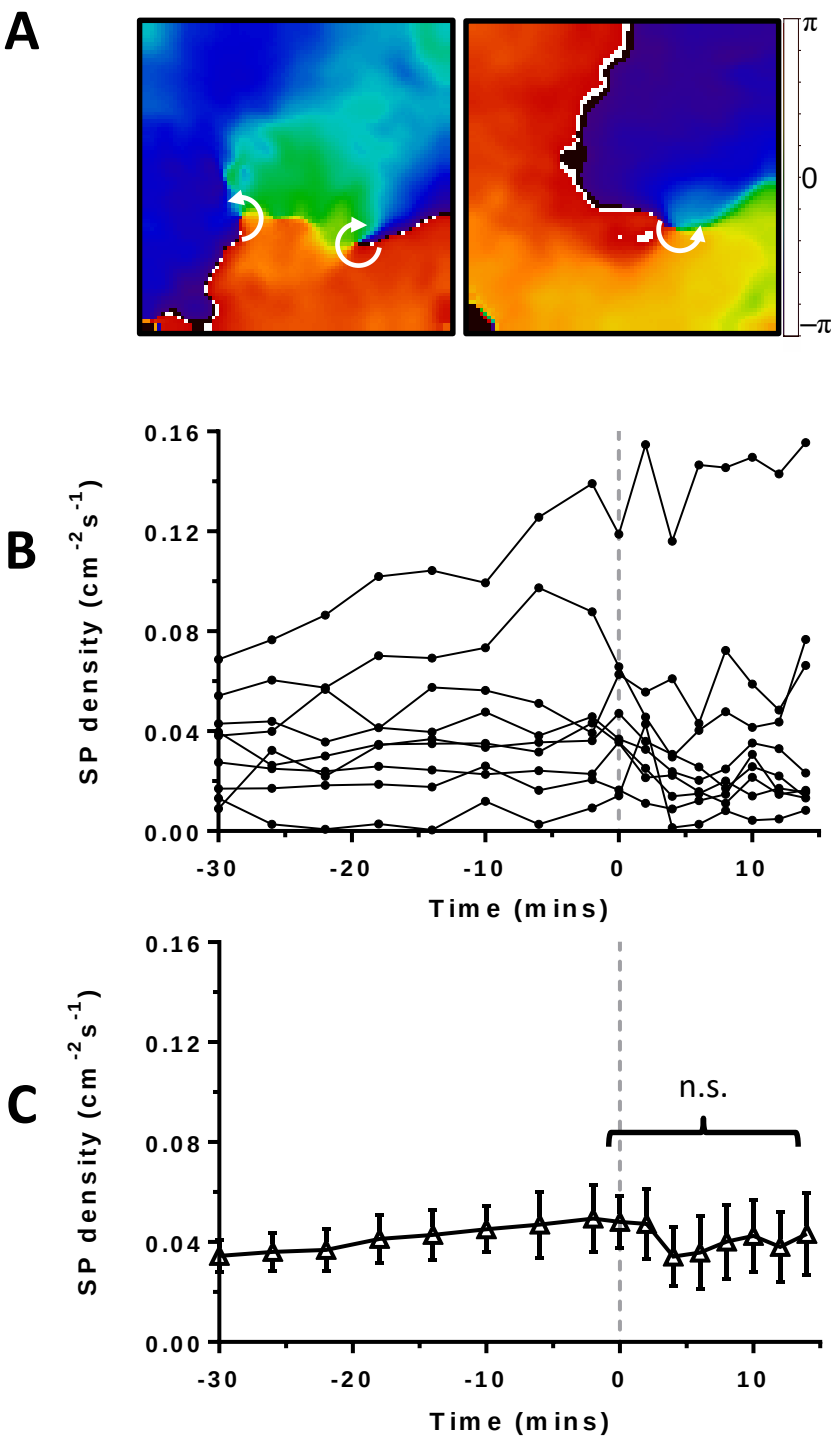


**Figure 5. Effect of ranolazine on singularity point (SP) density in tachypacing-induced persistent AF on the LA epicardium from perfused hearts. (A)** Representative phase maps of the LA epicardium before (left) and during (right) perfusion with ranolazine shows multiple rotors (white arrows indicate direction of rotation around SP). **(B)** Time course of SP density during persistent AF in 9 sheep hearts. Continuous perfusion with ranolazine (10 µM) begins at time 0 (dashed line). **(C)** Average SP density is not changed during perfusion with ranolazine.

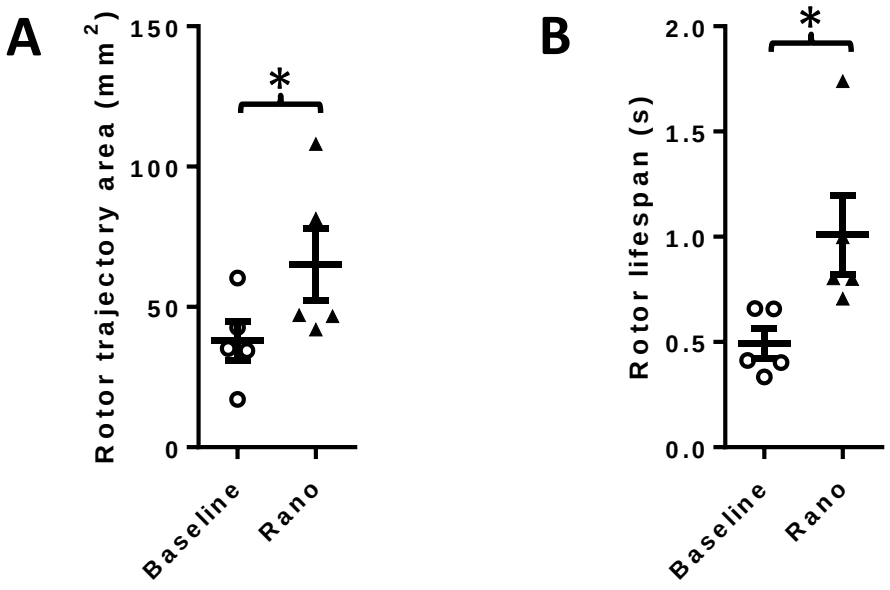


**Figure 6. Effect of ranolazine on rotor trajectory area and rotor lifespan on the LA epicardium from perfused hearts in tachypacing-induced persistent AF. (A)** Rotor trajectory areas significantly increased in the presence of ranolazine. **(B)** Rotor lifespans were significantly prolonged during perfusion with ranolazine (* $p<0.05$).

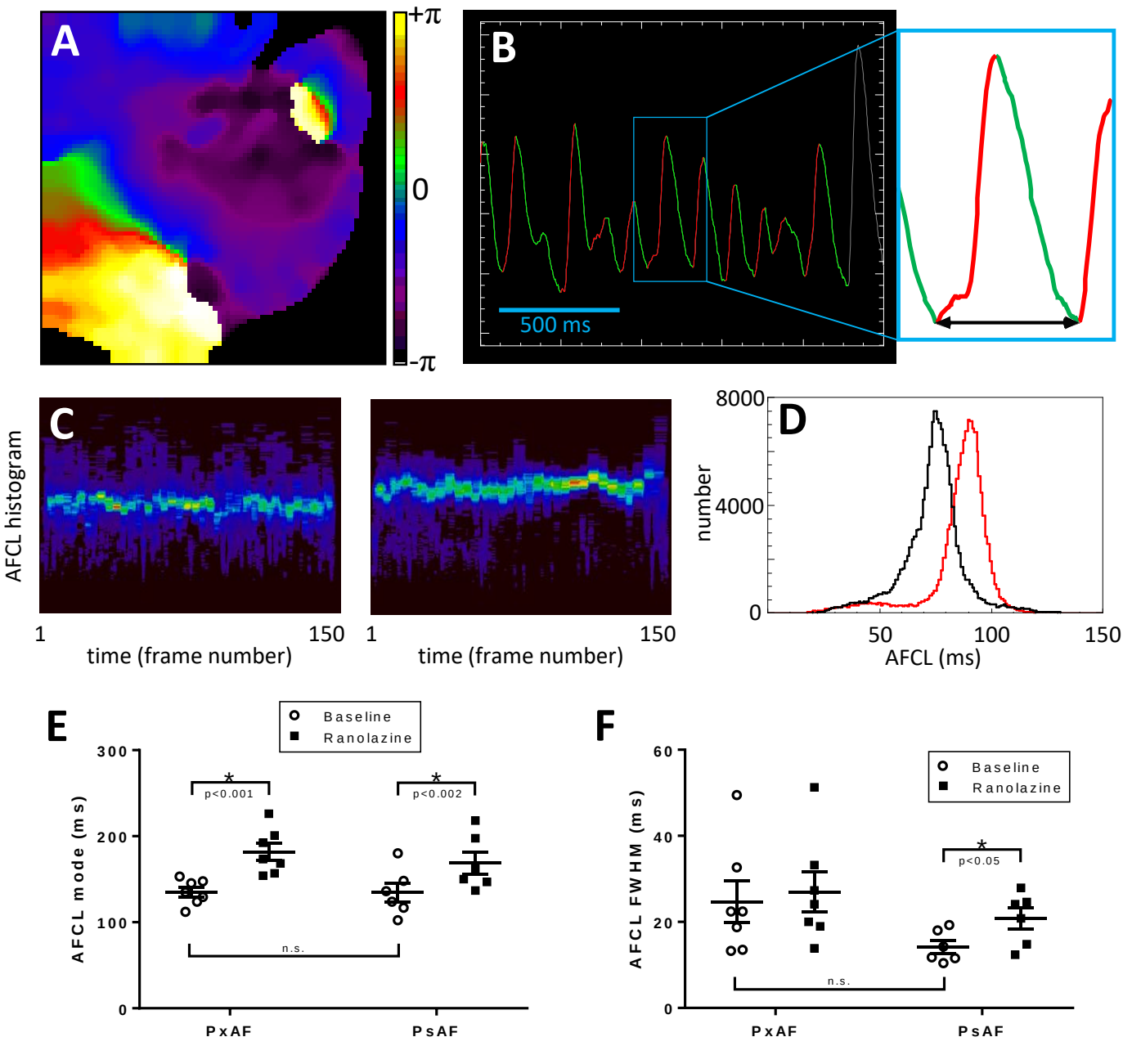


**Figure 7 AF cycle length (AFCL) during stretch-induced paroxysmal (Px) and tachypacing-induced persistent (Ps) AF. (A)** Representative phase map during PsAF. **(B)** Representative single-pixel optical voltage recording during PsAF displaying automated detection of upstroke (red) and downstroke (green). AFCL is measured for each activation between consecutive nadirs (arrow in inset). For each movie frame a histogram is constructed to measure AFCL distribution. **(C)** All histograms from a movie are stacked vertically into 3D histograms with brighter colours representing count numbers. Left and right panels show representative stacked histograms of PsAF before and during application of ranolazine, respectively. For each movie, stacked histograms are averaged across all frames. **(D)** Representative average AFCL histograms from the same heart in PsAF before (black) and during (red) application of ranolazine show prolongation of mean and mode AFCL with ranolazine. **(E)** Quantification of AFCL shows ranolazine prolonged AFCL in both PxAF and PsAF. **(F)** Quantification of full width at half maximum (FWHM) as an index of variance of average AFCL histograms (lines indicate mean±SEM).

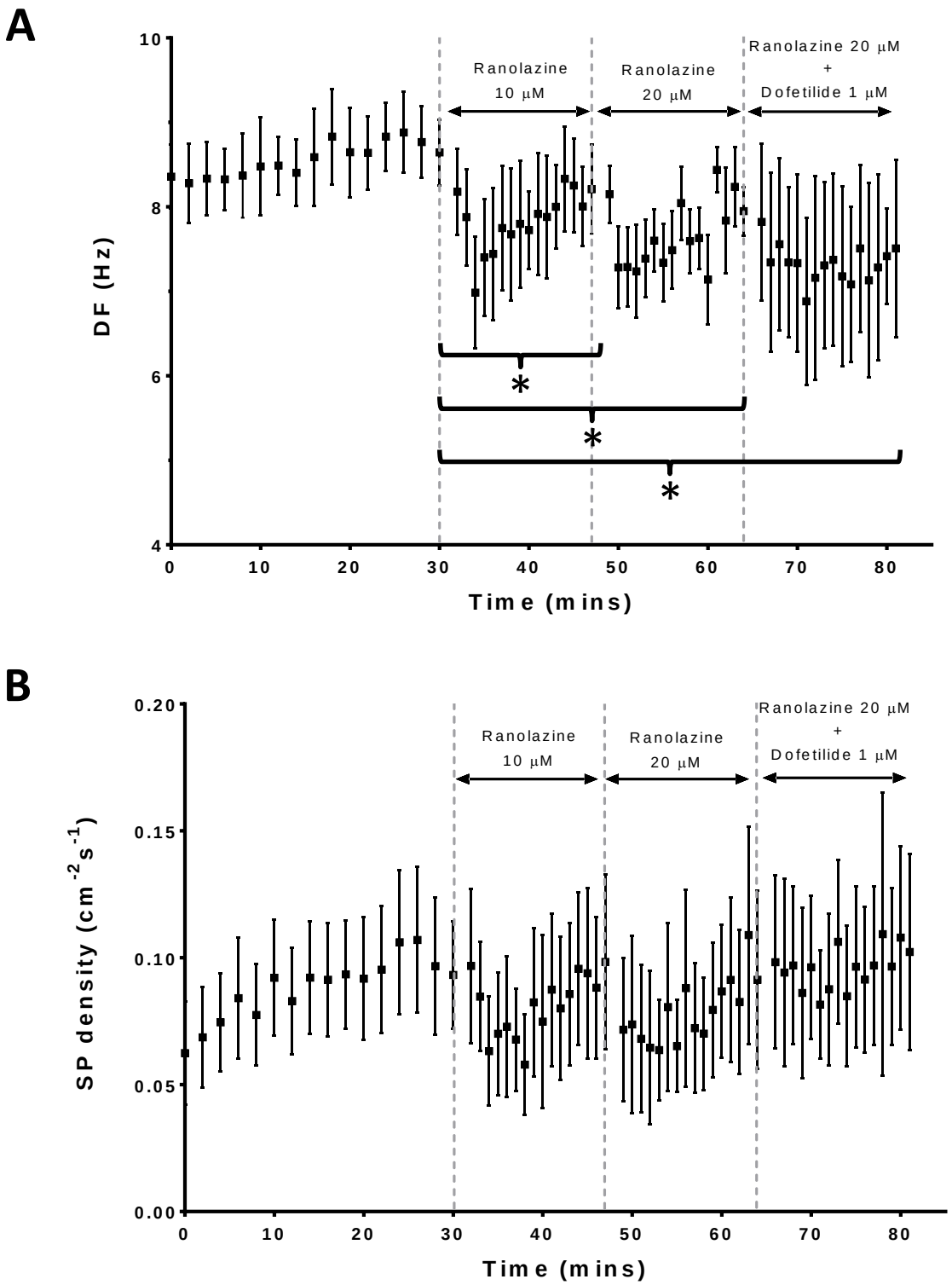


**Figure 8. Effects of ranolazine and dofetilide in persistent AF. (A)** In hearts from 5 sheep with tachypacing-induced persistent AF, after at least 30 minutes of baseline AF, 10 μM ranolazine was added to the perfusate for 15 minutes, followed by an increase in ranolazine concentration to 20 μM for 15 minutes, and lastly the addition of dofetilide (1 μM). The addition of dofetilide to ranolazine (20 μM) did not terminate persistent AF in any of the hearts despite decreasing average DF on the LA epicardium (* $p$<0.05 versus end of baseline). **(B)** The higher concentration of ranolazine plus dofetilide did not significantly change average SP density on the LA epicardium ($p$=n.s. versus end of baseline).

# Supplemental Material

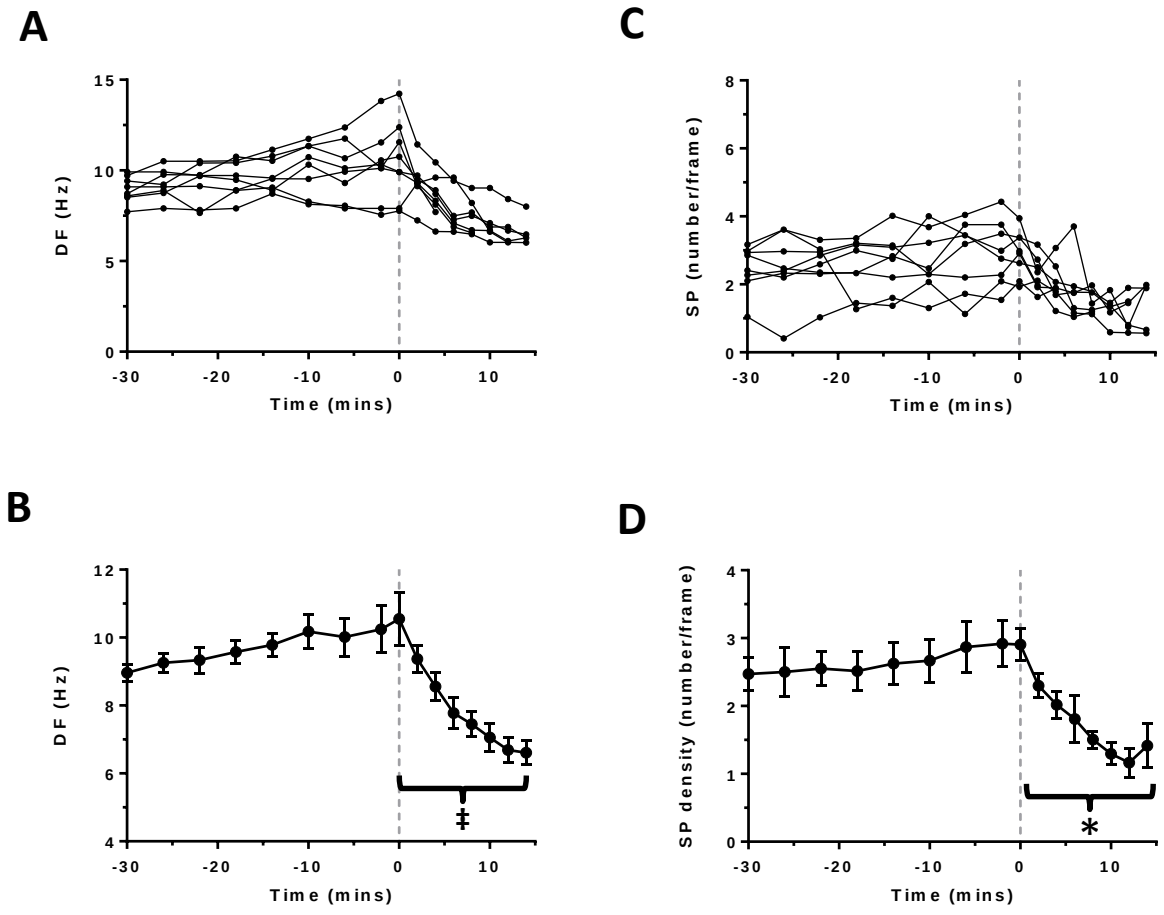


**Supplemental Figure S1. Effect of ranolazine on DF and singularity point (SP) density on posterior LA endocardium during stretch-induced paroxysmal AF in isolated hearts. (A)** Time course of maximum dominant frequency (DF) during paroxysmal AF (*N*=8). Continuous perfusion with ranolazine begins at time 0 (dashed line). **(B)** Average DF is significantly decreased during perfusion with ranolazine (‡$p$<0.002). **(C)** Time course of SP density during paroxysmal AF (*N*=8). At time 0 mins (dashed line) 10 µM ranolazine is added to the perfusate. **(D)** Average SP density is decreased (*$p$<0.001) during perfusion with ranolazine.

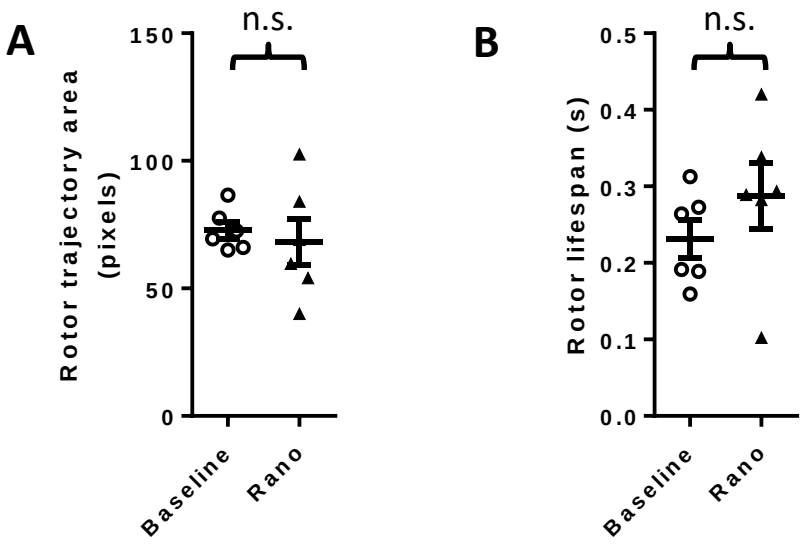


**Supplemental Figure S2. Effect of ranolazine on rotor trajectory area and rotor lifespan on posterior LA endocardium during stretch-induced paroxysmal AF. (A)** Rotor trajectory areas and **(B)** rotor lifespans were not significantly changed from baseline during perfusion with ranolazine (*p*=n.s., *N*=6).

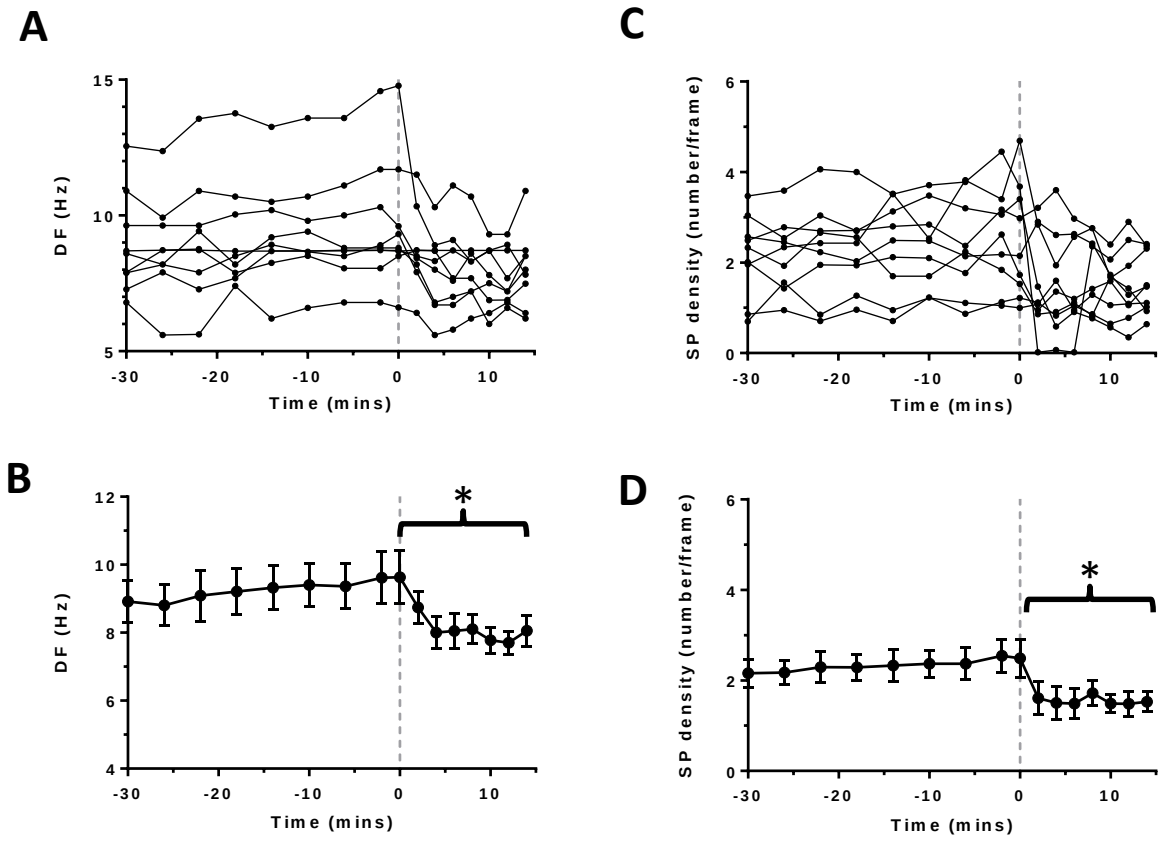


**Supplemental Figure S3. Effect of ranolazine on DF and singularity point (SP) density on posterior LA endocardium in tachypacing-induced persistent AF hearts. (A)** Time course of maximum dominant frequency (DF) during persistent AF (*N*=9). Continuous ranolazine perfusion begins at time 0 (dashed line). **(B)** Average DF is significantly decreased during perfusion with ranolazine (**p*<0.05). **(C)** Time course of SP density during persistent AF (*N*=9). At time 0 mins (dashed line) 10 μM ranolazine is added to the perfusate. **(D)** Average SP density is decreased (**p*<0.05) during perfusion with ranolazine.

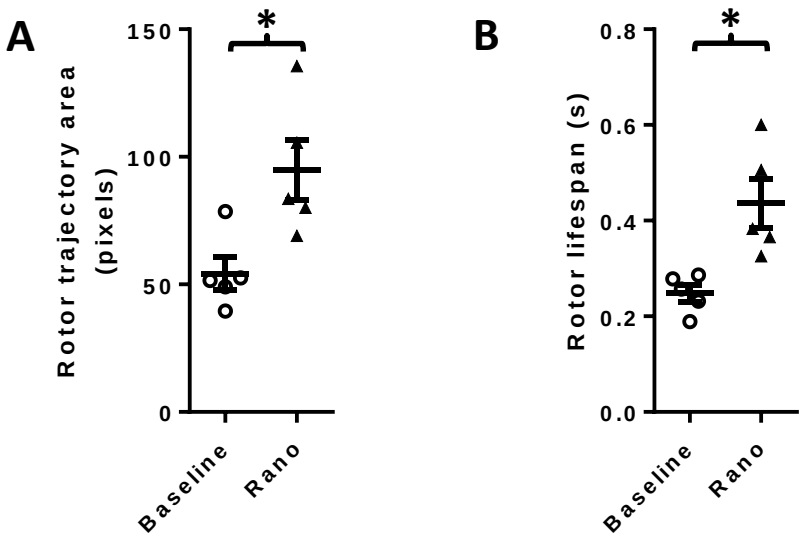


**Supplemental Figure S4. Effect of ranolazine on rotor trajectory area and rotor lifespan on posterior LA endocardium in tachypacing-induced persistent AF hearts. (A)** Rotor trajectory areas and **(B)** rotor lifespans were significantly increased from baseline during perfusion with ranolazine (**p*<0.05, *N*=5).

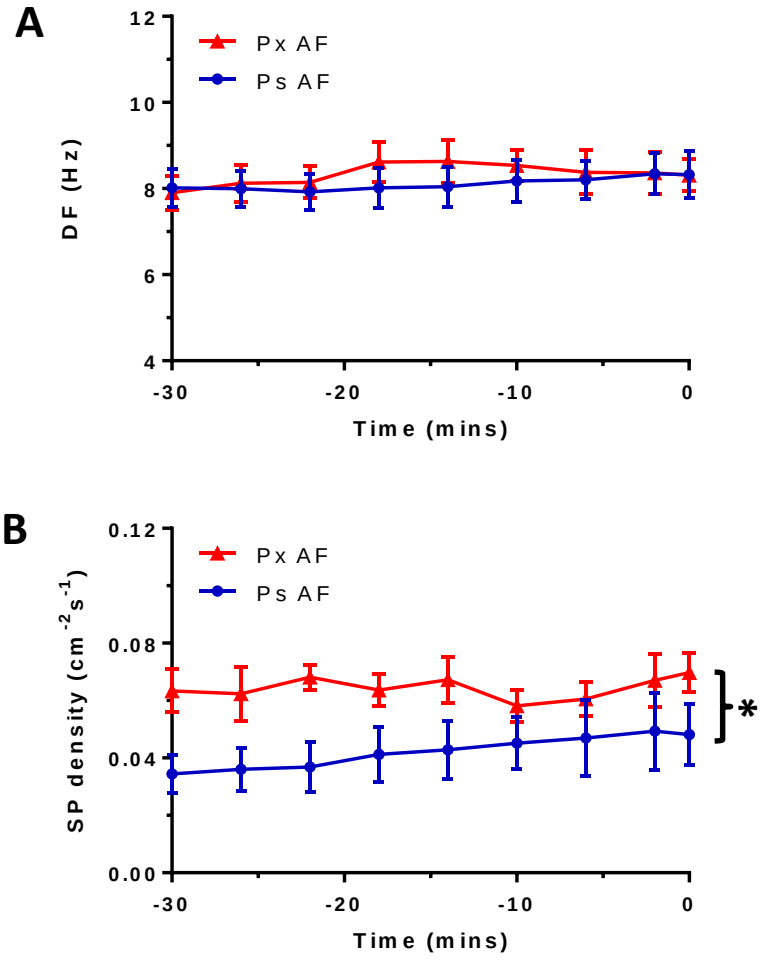


**Supplemental Figure S5. Rotor dynamics in paroxysmal (Px) and persistent (Ps) AF. (A)** Time course of average maximum dominant frequency (DF) during baseline AF. Mean baseline DF was not significantly different between Px and Ps AF. **(B)** Time course of average singularity point (SP) density during baseline AF. Mean SP density during 30 minutes of baseline AF was 0.064±0.001 $cm^{-2}s^{-1}$ during Px AF and was significantly lower (*****$p$<0.0001) during Ps AF with a value of 0.042±0.002 $cm^{-2}s^{-1}$.

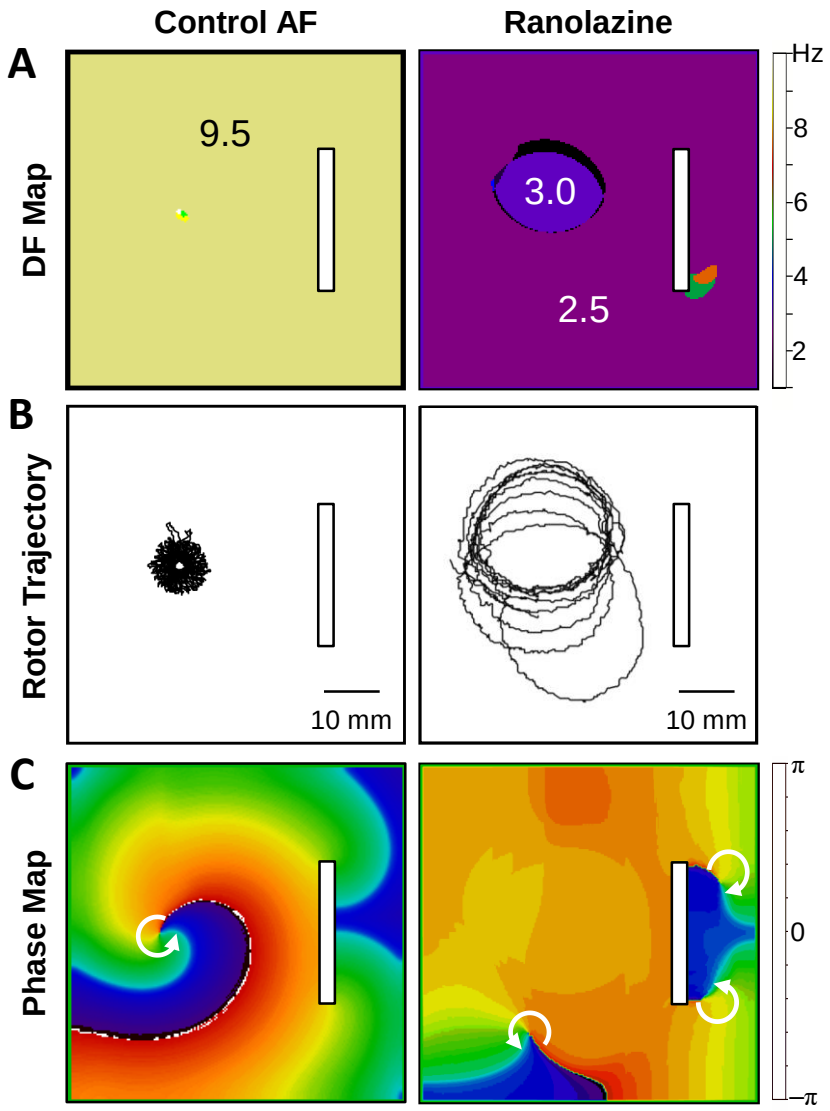


**Supplemental Figure S6. Computational simulations of sheep atrial rotors.** Numerical simulations of sheep atrial rotors were employed to provide further insights into the effects of ranolazine on rotor dynamics in an atrial AF substrate. AP propagation was simulated in 2-dimensional sheets during control AF conditions (left panels) and with reduced excitability simulating effects of ranolazine on $I_{Na}$ (right panels). The white rectangle represents a nonconducting, unexcitable obstruction. **(A)** DF maps show ranolazine decreased DF by reducing excitability, but **(B)** increased rotor trajectory area from 73.5 $mm^2$ (left) to 145.0 $mm^2$ (right). **(C)** Phase maps show that rotors remained attached to the distal side of the obstruction under control AF conditions (left), but the simulated effects of ranolazine resulted in vortex shedding and formation of new singularity points (right).